Optical Doppler Tomography for Noninvasive Imaging of *in vivo* Blood Flow

Zhongping Chen, T. E. Milner, S. Srinivas, T. Lindmo†, D. Dave, and J. Stuart Nelson
Beckman Laser Institute and Medical Clinic, University of California, Irvine, CA 92612
†Dept. of Physics, Norwegian University of Science and Technology, 7034 Trondheim, Norway

ABSTRACT

We report the development of an optical technique for noninvasive *in vivo* imaging of tissue structure and blood flow dynamics with high spatial resolution (2-15 μm) in biological systems. The technique is based on coherence optical Doppler tomography (ODT), which combines Doppler velocimetry with optical coherence tomography to measure blood flow velocity at discrete spatial locations. The exceptionally high resolution of ODT allows noninvasive *in vivo* imaging of both blood microcirculation and tissue structures surrounding the vessel, which has significance for biomedical research and clinical applications. Tomographic velocity imaging of *in vivo* blood flow in a rat mesentery is demonstrated.

Keywords: optical Doppler tomography, optical coherence tomography, blood flow imaging, laser Doppler velocimetry.

1. INTRODUCTION

Noninvasive techniques for imaging *in vivo* blood flow are of great value for biomedical research and clinical diagnostics [1]. The ideal microvascular imaging technique must fulfill several requirements: a) probe the underlying microcirculation at a user-specified depth in both superficial and deep layers; b) distinguish arterial from venous flow; c) detect blood flow changes rapidly; and d) be safe, noninvasive, reliable, and reproducible. Numerous approaches have been investigated including Doppler ultrasound [2], conventional angiography [3], laser Doppler flowmetry (LDF) [4], and magnetic resonance angiography [3]. Each of these techniques has limitations. Conventional LDF, for example, has been used to measure mean blood perfusion in the peripheral microcirculation. However, strong optical scattering in biological tissue limits spatially resolved flow measurements by LDF. Although Doppler ultrasound imaging provides a means to resolve flow velocities at different locations in a scattering medium, the relatively long acoustic wavelength required for deep tissue penetration limits spatial resolution to approximately 200 μm.

We report here the development of an optical technique for noninvasive *in vivo* imaging of blood flow dynamics and tissue structures with high spatial resolution (2-15 μm). The technique, optical Doppler tomography (ODT) [5], combines Doppler velocimetry with optical coherence interferometry to measure blood flow velocity at discrete spatial locations. The exceptionally high resolution of ODT allows noninvasive simultaneous imaging of both *in vivo* blood microcirculation and tissue structures surrounding the vessel. Tomographic imaging of *in vitro* flow using reconstituted canine blood and *in vivo* blood flow in the rodent mesentery are demonstrated.

2. OPTICAL DOPPLER TOMOGRAPHY

ODT combines LDF with optical coherence tomography [6-8] to obtain high resolution tomographic images of static and moving constituents in highly scattering biological tissues. ODT

SPIE Vol. 2981 • 0277-786X/97/$10.00

measures the amplitude and frequency of the interference fringe intensity generated between reference and target arms of a Michelson interferometer for structural and velocity images. High spatial resolution is possible because light backscattered from the sample recombines with the reference beam and forms interference fringes only when the optical path length difference is within the coherence length of the source light. When light backscattered from a moving constituent interferes with the reference beam, beating at the Doppler frequency occurs (Δf_D):

$$\Delta f_D = \frac{1}{2\pi}(\mathbf{k}_s - \mathbf{k}_i) \bullet \mathbf{v} \qquad (1)$$

where, $\mathbf{k}_i$ and $\mathbf{k}_s$ are wave vectors of incoming and scattered light respectively, and $\mathbf{v}$ is the velocity vector of the moving particle. With knowledge of the angle between the scattering vectors ($\mathbf{k}_s$-$\mathbf{k}_i$) and the velocity ($\mathbf{v}$), measurement of the Doppler frequency shift (Δf_D) allows determination of particle velocity at discrete user-specified locations in a turbid sample.

3. MATERIALS AND METHODS

3.1. ODT Instrument

The ODT instrument (Fig.1) uses a fiber optic Michelson interferometer with a superluminescent diode (λ_O=850 nm, $\Delta\lambda_{FWHM}$=25 nm) as the light source. The sample and reference mirrors constitute the two arms of the interferometer. Light from the SLD and an aiming beam (He-Ne laser, λ=633 nm) are coupled into a fiber interferometer using a 2x1 coupler and then split equally into reference and target arms of the interferometer by a 2x2 fiber coupler. Piezoelectric cylinders are used to modulate the optical path length of light in the reference and target arms by stretching the fiber wrapped around the cylinders. A ramp electrical wave (80 Hz) is used to drive the piezoelectric cylinders to generate optical phase modulation for the interference fringes (f_O=1600 Hz). Light in the sample path is focused onto the turbid sample by a gradient index lens (NA=0.2) with the optical axis oriented at 15° from the surface normal. ODT structural and velocity images are obtained by sequential lateral scans of the sample probe (i.e., fiber tip and gradient index lens) at constant horizontal velocity (800 μm/s) followed by linear incremental movement along the surface normal.

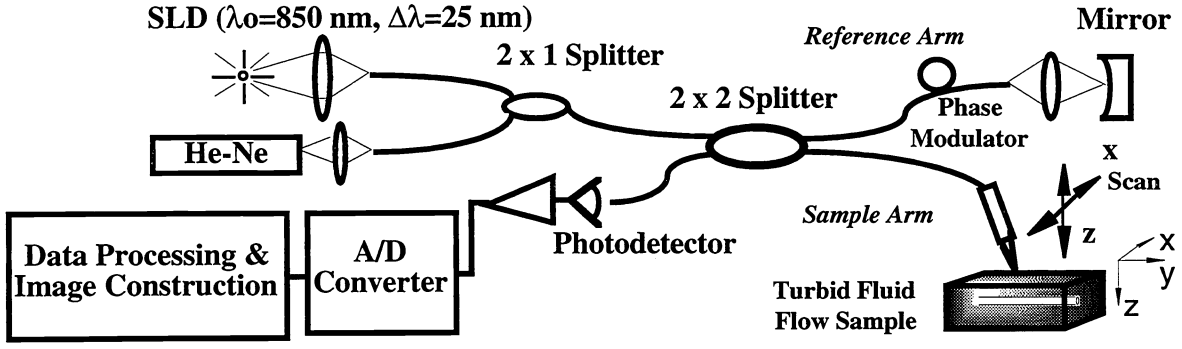

Fig. 1. Prototype instrument to measure ODT temporal interference fringe intensity.

To maintain the coherence gate at the beam waist position in the turbid sample, a dynamic focus-tracking technique is used. In this method, for each incremental movement (δ_1) of the sample probe along the surface normal, the reference mirror is translated (δ_2) to compensate for the new beam waist

position in the turbid sample. By requiring the coherence gate to be at the position of the beam waist, a relationship between δ_1 and δ_2 is derived from geometrical optics,

$$\delta_2 = \delta_1(\bar{n}^2 - 1) \tag{2}$$

where $\bar{n}$ is mean refractive index of the turbid sample. Dynamic focus-tracking not only maintains lateral spatial resolution when probing deeper positions, but also increases signal to noise ratio.

Light backscattered from the turbid sample is coupled back into the fiber and forms interference fringes at the photodetector. Temporal interference fringe intensity ($\Gamma_{ODT}(\tau)$) is measured by a single element silicon photovoltaic detector, where τ is the time delay between light from the reference and sample arms, and is related to the optical path length difference (Δ) between the two by $\tau=\Delta/c$. High axial spatial resolution is possible because interference is observed only when τ is within the source coherence time τ_c, or equivalently, when Δ is within the source coherence length ($L_c=\tau_c c$). The interference fringe signal is amplified, high passed, digitized (20 kHz) with a 16-bit analog-to-digital (A/D) converter, and transferred to a computer workstation for data processing. Signal processing algorithms to obtain velocity and structural images are illustrated in Fig. 2.

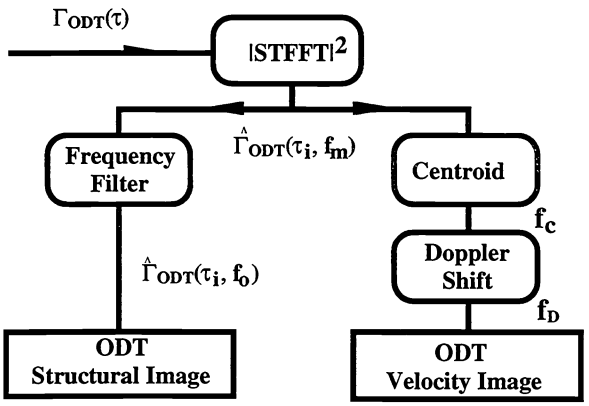

Fig. 2. Signal processing algorithms to obtain ODT structural and velocity images.

Spectrogram of interference fringe intensity at time delay τ_i and frequency f_m is calculated using short-time fast Fourier transform (STFFT):

$$\hat{\Gamma}_{ODT}(\tau_i, f_m) = \left|STFFT\left(f_m; \Gamma_{ODT}(\tau_i)\right)\right|^2 \tag{3}$$

A spectrogram is an estimate of the power spectrum of the temporal interference fringe intensity ($\hat{\Gamma}_{ODT}(\tau_i, f_m)$) in the i'th time delay window (τ_i , $\tau_i + \Delta\tau_o$), where τ_i is the delay of light in reference arm which determines the depth position (z_i) to be probed in the sample, and $\Delta\tau_o$ corresponds the data acquisition time window for each pixel. In our setup, information in the axial direction is obtained by incremental movement of the sample arm followed by focus tracking, and τ_i therefore denotes the i'th pixel to be probed.

A tomographic structural image is obtained by calculating the relative reflectivity which equals the value of the spectrogram at the phase modulation frequency (f_o). Because magnitude of the temporal interference fringe intensity decreases exponentially with increasing depth in the turbid sample, a logarithmic scale is used to display the ODT structural images:

$$S_{ODT}(i) = 10 \cdot \log\left(\hat{\Gamma}_{ODT}(\tau_i, f_o)\right) \quad (4)$$

Fluid flow velocity at each pixel is calculated by the Doppler frequency shift (Δf_D), which is determined by the difference between the carrier frequency established by the optical phase modulation (f_o) and the centroid (f_c) of the measured spectrogram at the each pixel:

$$v_{ODT}(i) = \frac{\lambda_o \Delta f_D}{2\cos(\theta)} = \frac{\lambda_o (f_c - f_o)}{2\cos(\theta)} \quad (5)$$

where we have assumed, $\mathbf{k}_s = -\mathbf{k}_i$ and θ is the angle between $\mathbf{k}_i$ and $\mathbf{v}$ in the air. The centroid of the measured power spectrum at each pixel is given by:

$$f_c = \sum_m f_m \hat{\Gamma}_{ODT}(\tau_i, f_m) / \sum_m \hat{\Gamma}_{ODT}(\tau_i, f_m) \quad (6)$$

Lateral and axial spatial resolutions of our ODT instrument are limited by the beam spot size and source coherence length (L_c) to 5 and 13 μm, respectively; higher axial resolution may be achieved by using a low coherence source with greater bandwidth. Velocity resolution in our prototype instrument (100 μm/s) is dependent on pixel acquisition time and the angle (θ) between flow velocity ($\mathbf{v}$) and the incoming light direction ($\mathbf{k}_i$). Velocity resolution may be improved with a smaller angle (θ) or longer pixel acquisition time. Using our prototype instrument, the approximate time to record simultaneously ODT structural and velocity images is 3 minutes (e.g., 1 × 1 mm^2, 5 × 13 μm^2 resolution).

3.2. Materials and Subjects

Canine blood was chosen as an *in vitro* model system to simulate the optical properties (i.e., absorption and scattering coefficients) of human blood [9]. Human and canine erythrocytes (red blood cells (RBCs)) have diameters of 7.8 and 7.2 μm, and thicknesses of 2.06 and 1.95 μm, respectively.

To avoid instability of imaging results due to gradual hemolysis during the experimental procedure, canine RBCs were fixed with glutaraldhyde to yield a stock suspension of single cells that could be reconstituted at any desired volume ratio of cells (i.e. hematocrit value). Briefly, packed canine RBCs (Hemopet, Irvine, CA) were aliquoted into 50 ml centrifuge tubes and diluted by adding twice the volume of cold PBS. After careful resuspension, the cells were centrifuged for 10 min at 300 g. This washing procedure was repeated three times. All resuspended aliquots were then put together and an equal volume of 1% glutaraldehyde (Ted Pella Inc, Redding, CA) in cold PBS was added, resulting in 0.5% glutaraldhyde concentration in a suspension of about 15 % cells by volume. After 2 hours of fixation at 4°C on a tilting table (12 periods/min), the cells were aliquoted out and washed three times in cold PBS with 0.1% azide. The RBCs were finally resuspended in azide-supplemented autologous plasma at a nominal volume fraction of 50 % and stored at 4°C. A stock suspension of fixed RBCs in autologous plasma was diluted 16 times in fetal calf serum right before ODT measurement. Inspection of the final suspensions by microscopy showed a high fraction (>90%) of single cells.

The rodent mesentery model is used to demonstrate the potential of ODT for *in vivo* imaging of vascular blood flow in different organs. A rodent (rattus norvegicus) was anesthetized and a loop of small intestine was exposed through an abdominal incision to allow access to the mesenteric vasculature.

4. RESULTS AND DISCUSSION

4.1. *In vitro* Results

To demonstrate the ability of our ODT instrument for imaging blood flow, we first look at the in vitro system consisting of reconstituted blood flow in a plastic tubing submerged in a scattering phantom of intralipid. ODT images were obtained when a suspension of reconstituted canine blood was infused at constant velocity through a circular polyethylene conduit (inner diameter 375 μm) submerged in a highly scattering 1% intralipid solution. In the structural images (Fig. 3A), the gray scale change from white at the surface to darker shades at deeper positions indicates strong attenuation of the temporal interference fringe intensity due to scattering in the turbid sample. Dynamic range of the temporal interference fringe intensity power spectrum is 60 dB. Backscattered light from the conduit wall is evident. Lumen appears dark because temporal interference fringe intensity of light backscattered from flowing RBC is Doppler shifted (Δf_D) with respect to the phase modulation frequency (f_o) and does not contribute to the power spectrum at frequency f_o. In the ODT velocity image (Fig. 3B), static regions in the conduit appear dark (V=0), while the presence of RBC moving at different velocities is evident. RBC near the center of the conduit are observed to move faster than those near the circular wall. A horizontal cross section of the velocity profile through the center of the conduit is shown in Fig. 3C, where the open circles are the experimental data and the solid line is a theoretical fit assuming laminar flow with a known inner conduit diameter. Agreement between theory and experiment suggests laminar flow as expected.

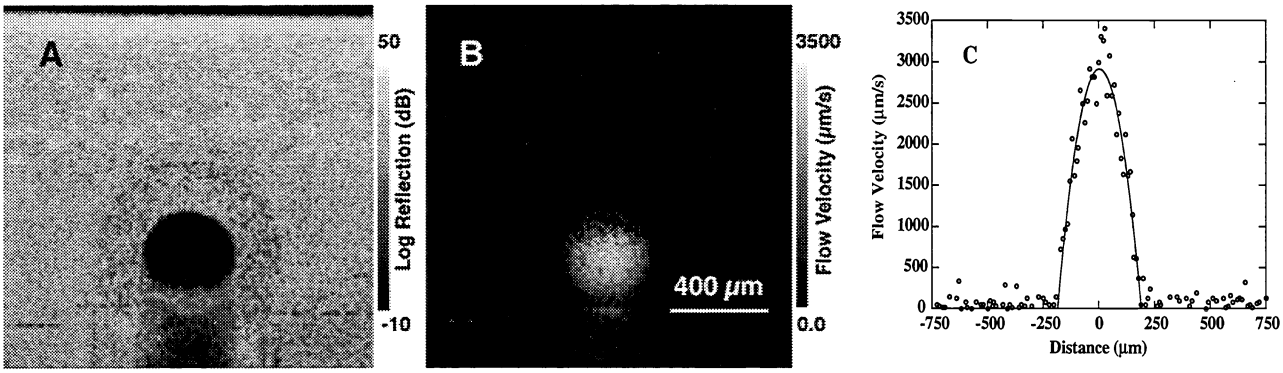

Fig. 3. ODT images of flowing reconstituted canine blood in a circular conduit (inner diameter 375 μm) submerged in a highly scattering phantom of 1% intralipid solution. A: ODT structural image; B: ODT velocity image; C: Velocity profile along a horizontal cross section passing through the center of conduit.

4.2 *In vivo* Results

To investigate the ability of our ODT instrument to image *in vivo* blood flow in biological tissues, *in vivo* mesentery blood flow in both veins and arteries was imaged using ODT (Fig. 4). Structural (Fig. 4A) and velocity images (Figs. 4B and C) were obtained simultaneously. The presence of vessel-like circular features can be observed in the structural image (Fig. 4A). Velocity images of blood flow moving in opposite directions, as determined by the sign of the Doppler frequency shift, are shown in Figs. 4B and C. Here static structures (v=0) in the mesentery appear dark, while blood flow in both veins and arteries appears as lighter shades. Blood flow in two small veins and a small artery with diameter of approximately 100 μm, are clearly identified. Velocity profile along a horizontal cross

section passing through both vein and artery at a depth corresponding to the left arrow indicated in Fig. 4A is shown in Fig. 4D.

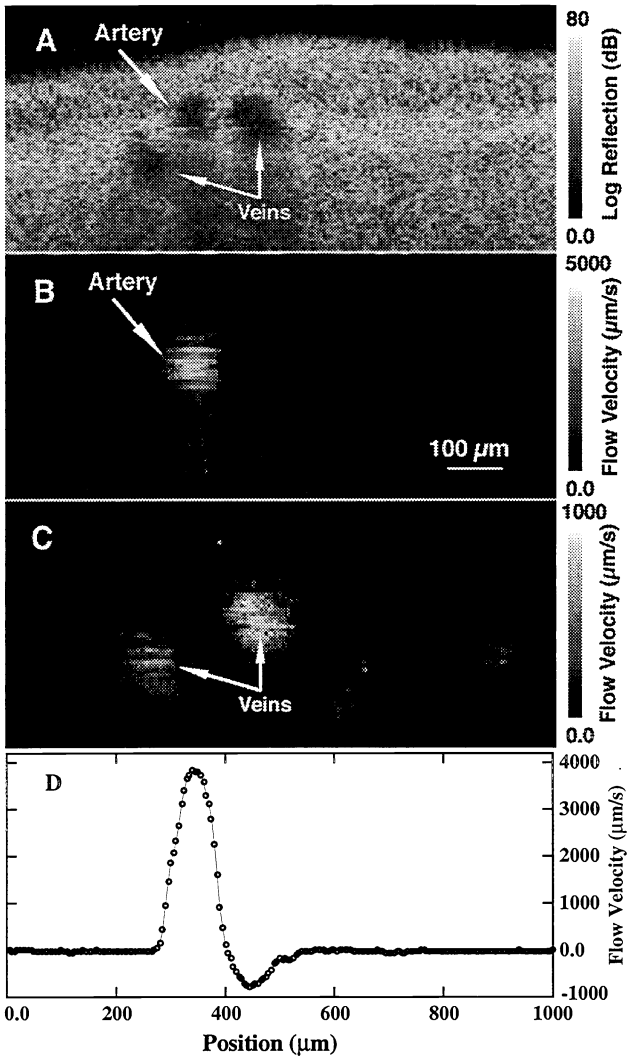

Fig. 2. ODT images of *in vivo* blood flow in the vasculature of rat mesentery. A: structure images; B: arterial flow velocity image; C: venous flow velocity image; D: velocity profile along a horizontal cross section passing through both vein and artery at a depth corresponding to the left arrow indicated in A.

These results demonstrate that ODT offers a noninvasive method to image *in vivo* blood flow dynamics and tissue structure surrounding the flow. The exceptionally high spatial resolution of ODT has broad implications for the clinical management of patients where blood flow monitoring is essential. The importance of noninvasive imaging of the microvasculature in reconstructive surgery is underscored by the reported high salvage rates of failing flaps and replants (60-80%). Information provided by the ODT images can be used to determine tissue perfusion and viability before, during, and after surgical reconstructive procedures; assess the efficacy of pharmacological intervention for failing surgical flaps or replants; evaluate the skin microcirculation for a variety of lesions before, during and after treatment; and investigate the mechanism of photodynamic therapy for cancer treatment.

5. SUMMARY

We have developed an ODT system for noninvasive imaging of in vivo blood flow. We demonstrated in *in vitro* and *in vivo* studies on turbid samples and model vasculatures, respectively, the feasibility and potential application of ODT to image and characterize blood flow with high spatial resolution at discrete user-specified locations in highly scattering biological tissues. ODT is noninvasive and noncontact, and possesses exceptional spatial resolution (2-15 μm). ODT is not only a promising technique for noninvasive in vivo imaging of blood flow velocity, but also can be applied to other areas where rapid and noninvasive monitoring of turbulent or laminar flow in scattering media is essential.

6. ACKNOWLEDGMENT

Authors wish to thank M. J. C. van Gemert and D. J. Smithies for helpful discussions. This project is supported by research grants awarded from the Biomedical Research Technology Program and Institute of Arthritis and Musculoskeletal and Skin Diseases (1R29-AR41638-01A1 and 1R01-AR42437) at the National Institutes of Health, Whitaker Foundation, and Dermatology Foundation. Institute support from Department of Energy, National Institutes of Health, and Beckman Laser Institute Endowment is also gratefully acknowledged.

7. REFERENCES

[1]. E. Yamada, M. Matsumura, S. Kyo, and R. Omoto, "Usefulness of a prototype intravascular ultrasound imaging in evaluation of aortic dissection and comparison with angiographic study, transesophageal echocardiography, computed tomography, and magnetic resonance imaging," *Am. J. Cardiol.*, vol. 75, pp. 161-165, 1995.

[2]. J. V. Chapman, in *The Noninvasive Evaluation of Hemodynamics in Congenital Heart Disease*, Chap. 2, J. V. Chapman and G. R. Sutherland, Eds. Dordrecht, The Netherlands: Kluwer, 1990, pp. 57.

[3]. W. J. Manning, W. Li, and R. R. Edelman, "A preliminary report comparing magnetic resonance coronary angiography with conventional angiography," *N. Engl. J. Med.*, vol. 328, pp. 828-32, 1993.

[4]. R. F. Bonner and R. Nossal, in *Laser-Doppler Blood Flowmetry*, Chap. 2, A. P. Shepherd and P. A. Oberg, Eds. Dordrecht, The Netherlands: Kluwer, 1990, pp. 17.

[5]. Z. Chen, T. E. Milner, D. Dave, and J. S. Nelson, "Optical Doppler tomographic imaging of fluid flow velocity in highly scattering media," *Opt. Lett.*, vol. 22, pp. 64-66, 1997.

[6]. D. Huang, E. A. Swanson, C. P. Lin, J. S. Schuman, W. G. Stinson, W. Chang, M. R. Hee, T. Flotte, K. Gregory, C. A. Puliafito, and J. G. Fujimoto, "Optical Coherence Tomography," *Science*, vol. 254, pp. 1178-1181, 1991.

[7]. A. F. Fercher, "Optical coherence tomography," *J. of Biomedical Opt.*, vol. 1, pp. 157-173, 1996.

[8]. J. A. Izatt, M. R. Hee, E. A. Swanson, C. P. Lin, D. Huang, J. S. Schuman, C. A. Puliafito, and J. G. Fujimoto, "Micrometer-Scale Resolution Imaging Of The Anterior Eye In Vivo With Optical Coherence Tomography," *Archives Of Ophthalmology*, vol. 112, pp. 1584-1589, 1994.

[9]. C. M. Hawkey and T. B. Dennett, Color atlas of comparative veterinary hematology: normal and abnormal blood cells in mammals, birds and reptiles., 1 st ed. Ames: Iowa State University Press, 1989.